



LUND UNIVERSITY
Faculty of Medicine

LUP

Lund University Publications

Institutional Repository of Lund University

This is an author produced version of a paper published in *Physics in Medicine and Biology*. This paper has been peer-reviewed but does not include the final publisher proof-corrections or journal pagination.

Citation for the published paper:
Mårten Dalaryd, Gabriele Kragl, Crister Ceberg,
Dietmar Georg, Brendan McClean,
Sacha Af Wetterstedt, Elinore Wieslander,
Tommy Knöös

"A Monte Carlo study of a flattening filter-free linear accelerator verified with measurements."

Physics in Medicine and Biology 2010 55(23), 7333 - 7344

<http://dx.doi.org/10.1088/0031-9155/55/23/010>

Access to the published version may require journal subscription.

Published with permission from: Institute of Physics

A Monte Carlo study of a flattening filter-free linear accelerator verified with measurements

Mårten Dalaryd^{1,3}, Gabriele Kragl², Crister Ceberg³, Dietmar Georg², Brendan McClean⁴, Sacha af Wetterstedt⁵, Elinore Wieslander¹ and Tommy Knöös^{1,3}

¹ Radiation Physics, Skåne University Hospital and Lund University, Lund, Sweden

² Department of Radiotherapy, Medical University Vienna/AKH, Vienna, Austria

³ Medical Radiation Physics, Lund University, Lund, Sweden

⁴ Radiotherapy Department, St. Luke's Hospital, Dublin, Ireland

⁵ Department of Radiation Physics, Skåne University Hospital and Lund University, Malmö, Sweden

Email: marten.dalaryd@skane.se

Short title: Flattening filter-free linac studied by Monte Carlo

Abstract. A Monte Carlo model of an Elekta Precise linear accelerator has been built and verified by measured data for a 6 MV and 10 MV photon beam running with and without a flattening filter in the beam line. In this study the flattening filter was replaced with a 6 mm thick copper plate, provided by the linac vendor, in order to stabilize the beam. Several studies have shown that removal of the filter improves some properties of the photon beam, which could be beneficial for radiotherapy treatments. The investigated characteristics of this new beam included output, spectra, mean energy, half value layer and the origin of scattered photons. The results showed an increased dose output per initial electron at the central axis of 1.76 and 2.66 for the 6 MV and 10 MV beams, respectively. The number of scattered photons from the accelerator head was reduced by $(31.7 \pm 0.03) \%$ (1 SD) for the 6 MV beam and $(47.6 \pm 0.02) \%$ for the 10 MV beam. The photon energy spectrum of the unflattened beam was softer compared to a conventional beam and did not vary significantly with off-axis distance, even for the largest field size (0-20 cm off-axis).

1. Introduction

The flattening filter is introduced into conventional beam lines to provide uniform dose distribution at a clinical depth, usually 10 cm depth in water. The filter is a major contributor of scattered radiation in the treatment head (Chaney *et al* 1994, Fix *et al* 2001) and can lead to higher doses outside the treatment field (Kragl *et al* 2010, Kry *et al* 2010, O'Brien *et al* 1991). Due to the non-uniform shape of the flattening filter, the beam energy distribution will vary with off-axis distance, creating challenges for dose calculation algorithms. One way of removing these unfavourable properties of conventional clinical radiation beams would be to remove the flattening filter. Unflattened fields have, for small field sizes, dose profiles similar to those produced with a flattening filter in the beam line. This, along with the higher dose rate of unflattened fields, will increase the efficiency when delivering stereotactic radiosurgery (Vassiliev *et al* 2009, O'Brien *et al* 1991). For larger clinical targets the desired photon fluence could be modulated using the MLC and movable jaws allowing flattening filter-free beams to be a useful approach for the delivery of radiotherapy treatments (Vassiliev *et al* 2007). It has been suggested in the literature that removing the flattening filter would reduce the risk of secondary cancer incidence in IMRT-treatments (Hall 2007, Kry *et al* 2010). Dedicated IMRT-units, such as the TomoTherapy™ and Cyberknife™ units, already utilise these advantages by operating without flattening filter (Araki 2006, Jeraj *et al* 2004, Mackie *et al* 1993).

Several Monte Carlo studies of flattening filter-free (FFF) treatment machines have been published. A group at MD Anderson used measurement and Monte Carlo simulations to study a Varian linac where the flattening filter was replaced by a 2 mm thick copper plate (Vassiliev *et al* 2006, Titt *et al* 2006, Pönisch *et al* 2006, Kry *et al* 2010). Comparisons between photon beams produced with and without flattening filter in the beam line for an Elekta SL 25 linac using Monte Carlo simulations have also been reported earlier (Mesbahi and Nejad 2008, Mesbahi *et al* 2007).

We have previously published measurement data on flattening filter-free Elekta Precise linacs (Kragl *et al* 2009, Georg *et al* 2010). In the current work we present Monte Carlo simulated data, which support and complement our experimental studies for the 6 MV and 10 MV photon beams. In addition, Monte Carlo simulations extend our previous work towards quantities which are not readily measured but which will improve the understanding of the differences between beams with or without a flattening filter in the beam line.

In contrast with previous Monte Carlo studies of the same accelerator type this study presents data on a different linac model and an additional energy of 10 MV. The incident beam energy was tuned using measured data for both flattened and unflattened beams. Another novelty in the present Monte Carlo study is the insertion of a copper disk in the flattening filter-free beam line.

2. Material and methods

2.1. Experimental setting

Two Elekta Precise linear accelerators (Elekta Oncology Systems, Stockholm, Sweden) were modified to deliver flattening filter-free beams, one at St Luke's Hospital in Dublin, Ireland (SLH) and one at the Medical University of Vienna, Austria (MUW). A 6 mm thick copper plate was inserted into one of the filter carousel ports inside the treatment head. The filter was provided by the linac manufacturer but it is not necessary the type or thickness of filter that will be used in any possible future release of a flattening filter-free beam from Elekta. As a safety measure, the linac control system for the flattening filter-free beam was run on a separate removable hard drive, preventing it from being used clinically.

Both accelerators were equipped with asymmetric jaws and an MLC consisting of 40 leaf pairs producing 1 cm wide fields at isocentre and allowing a maximum field size of 40x40 cm² at the isocentre plane.

In this Monte Carlo study, two photon beam energies, 6 MV and 10 MV, were investigated. The 6 MV beam was from the linac at SLH and the 10 MV beam from MUW. In FFF-mode the incident electron energy was kept the same as for the flattened beams. The 6 MV flattening filter was about 2.5 cm thick at the central axis and made of steel and the 10 MV filter was about 2.3 cm thick and made out of tungsten and aluminium.

Depth dose and lateral profiles were measured using a PTW MP3 Water-Tank (PTW Freiburg, Germany) at SLH and an IBA Blue Phantom (IBA dosimetry Schwarzenbruck, Germany) at MUW. Depth dose profiles were measured with ionization chambers (PTW semiflex type 31010 at SLH and IBA CC13 at MUW) and lateral profiles using diodes (PTW type 60008 at SLH and IBA type SFD at MUW) (Kragl *et al* 2009).

2.2 Monte Carlo Simulations

Monte Carlo simulations were performed using the EGSnrc based user codes BEAMnrc and DOSXYZnrc (Rogers *et al* 1995, Kawrakow and Rogers 2002, Walters *et al* 2005, Rogers *et al* 2005). The Monte Carlo model of the accelerator head was built using explicit data from the vendor. A schematic illustration of the linac model is presented in figure 1. When tuning the properties of the incident electron beam, the electron and photon cut-off energies were set to 711 keV (ECUT) and 10 keV (PCUT), respectively. Electron range rejection was set to 2 MeV (ESAVE). The threshold for secondary particle production was set to ECUT for charged particles and PCUT for photons. Directional Bremsstrahlung Splitting (DBS) was used with a splitting number of 1000 and Russian roulette turned on. For all simulations bremsstrahlung angular sampling was performed using the full equation of Koch-Motz and the remaining parameters were set to their default values.

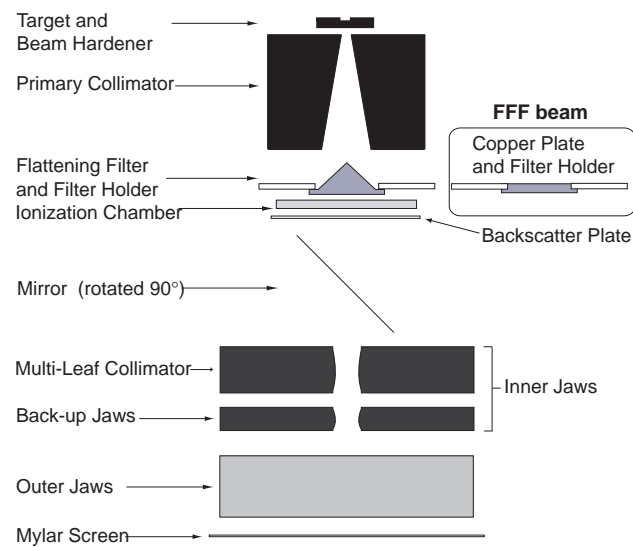


Figure 1. Overview of the linac-head components used in the Monte Carlo simulation. In the flattening filter position in the filter holder either a 6 MV or 10 MV flattening filter or, when running in flattening filter-free mode, a copper plate was positioned (not to scale).

For the tuning of the incident beam parameters, depth dose profiles for $10 \times 10 \text{ cm}^2$ fields and lateral profiles for $20 \times 20 \text{ cm}^2$ fields were compared to measurements for both flattened and unflattened fields. For the $10 \times 10 \text{ cm}^2$ fields, 4×10^7 histories were run in the accelerator head calculations, and 1×10^7 for $20 \times 20 \text{ cm}^2$ fields. A phase space was scored in a plane perpendicular to the beam axis at 90 cm distance from the target. Dose calculations in DOSXYZnrc were performed using a water phantom with the dimensions $50 \times 50 \times 50 \text{ cm}^3$ and the phantom was positioned at an SSD of 90 cm. The particles in each phase space were reused several times in order to achieve a statistical uncertainty (1 SD) below 0.5 % in voxels beyond the depth of maximum dose and within the field edges. For depth-dose calculations the voxel size was $0.5 \times 0.5 \text{ cm}^2$ in the lateral and longitudinal directions and 0.25 cm in depth. Lateral profiles were calculated with 0.25 cm resolution in the direction of interest and 0.5 cm in the remaining two dimensions.

The incident electron beam was varied by means of its mean energy, lateral spread in both inline (radial) and crossline (transversal) directions and mean angular spread. The width of the energy distribution of the electron beam was kept constant according to specifications by the linac vendor. The parameters were varied until both flattening filter-free and flattened beams agreed with measurements within 1.5 % for depth-dose profiles and 2 % for lateral profiles in local dose in the central part of the field and 4 % up to 5 cm outside the field.

For the calculation of phase space files needed for the extraction of beam properties, the tuned incident electron beam was used in a recalculation of the treatment head simulation of $40 \times 40 \text{ cm}^2$ and $20 \times 20 \text{ cm}^2$ fields using Uniform Bremsstrahlung Splitting (UBS) with a splitting factor

of 20 and Russian roulette turned off. For each field, $1 \cdot 10^9$ histories were run and a phase space was scored in air at isocenter level.

Information about particle energy, fluence, energy fluence and mean energy was extracted using the utility program BEAMDP. The last interaction point of the photons reaching the scoring plane was extracted using the ZLAST option in the BEAMnrc system (Rogers *et al* 2005). By using the LATCH variable, information about photons having interacted in the flattening filter or copper plate was extracted.

The off-axis variation in output was evaluated in $0.5 \times 0.5 \text{ cm}^2$ large square bins centred on the major axis parallel to the MLC at a depth of 10 cm and SSD 90 cm for a field size of $20 \times 20 \text{ cm}^2$.

Spectral composition was investigated at the central axis and at off-axis positions for the $40 \times 40 \text{ cm}^2$ fields, by scoring the photon energy distribution in two regions; one circle with a diameter of 1 cm with its centre on the central axis and one annulus with an inner radius of 17 cm and an outer radius of 18 cm at the isoplane.

The beam hardening effect was further investigated in terms of half-value layer (HVL) variation with off-axis distance. HVL was here defined as the thickness t of water needed to attenuate the in-air collision kerma K_c to half of its measure from when no absorber was present. In order to calculate this thickness equation (1) was applied. The summation was performed over 200 equidistant energy bins, with fluence $\left(\frac{\Delta\Phi}{\Delta E}\right)_i$, mid-energy E_i , and energy width ΔE_i . The linear attenuation coefficient μ and the mass energy absorption coefficient μ_{en}/ρ for each energy bin were taken from the XAAMDI database (X-ray Attenuation and Absorption for Materials of Dosimetric Interest) (Hubbell and Seltzer 1995). The primary photon fluence, i.e. photons not interacting in the collimator head, was scored in 10 annular bins with a width of 1 cm. Each of these bins was positioned so that the photons entering the middle of it had an angle to the central axis of one to ten degrees in steps of one degree. For the central axis HVL-value the fluence was scored in a circle centred at the central axis with a diameter of 1 cm.

$$K_c(t)/K_c(0) = \frac{\sum_{n=i}^N \left(\frac{\Delta\Phi}{\Delta E}\right)_i E_i \frac{\mu_{en,air}}{\rho}(E_i) \cdot \exp[-\mu(E_i)_{absorber} \cdot t] \Delta E_i}{\sum_{n=i}^N \left(\frac{\Delta\Phi}{\Delta E}\right)_i E_i \frac{\mu_{en,air}}{\rho}(E_i) \cdot \Delta E_i} = \frac{1}{2} \quad (1)$$

3. Results

3.1 Tuning of Monte Carlo parameters

For the 6 MV beam, a match between measurement and simulation was found for an incident electron beam with a mean energy of 6.6 MeV and a Gaussian energy spread of 0.5 MeV (FWHM). The focal spot size was 2.6 mm (FWHM) in the crossline direction and 0.6 mm (FWHM) in the inline direction with a mean angular spread of 0.8 degrees. For the 10 MV beam the corresponding values were 10.4 MeV, 0.3 MeV, 2.5 mm, 0.5 mm and 0.9 degrees. Depth doses and lateral profiles for the 6 MV and 10 MV beams with and without flattening filter are shown in figure 2 and 3, respectively. The agreement between measurements and calculations were within 1.5 % for depth dose profiles beyond the depth of maximum dose and within 2 % for lateral profiles within the central ± 9 cm. In the penumbral region the agreement was within 2 mm for the 6 MV beam and within 1 mm for the 10 MV. The out-of-field dose agreed within 4 % for all beams. These results were in coincidence with previous studies (De Smedt *et al* 2005, Sheikh-Bagheri and Rogers 2002). For the 10 MV beams in figure 3, the out-of-field-dose was lower for the calculated lateral profiles. This is due to the energy dependence of the unshielded diode used in the measurements. For ionization chamber measurements the doses outside the field agreed within the stated 4 %. The statistical uncertainty in each calculated voxel presented is within 0.4 % (1 SD) beyond the depth of maximum dose and inside the radiation field.

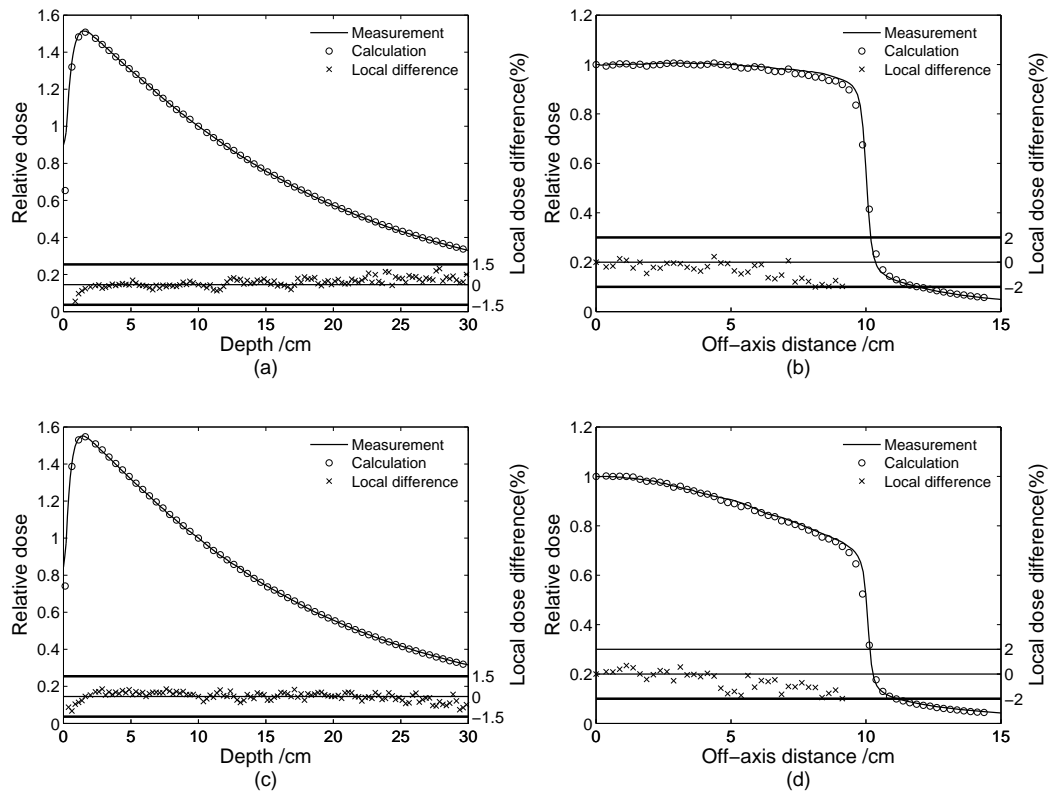


Figure 2. Comparisons of calculated and measured depth doses and lateral profiles at 6 MV. The percentage differences between measured and calculated dose values are shown at the bottom of the figures (right scale). Left: Depth dose distribution for 6 MV beams with (a) and without (c) a flattening filter for a $10 \times 10 \text{ cm}^2$ field with SSD 90 cm. The depth dose data were normalized to unity at 10 cm depth. Right: Lateral profiles with (b) and without (d) a flattening filter at 10 cm depth at an SSD of 90 cm for a $20 \times 20 \text{ cm}^2$ field. Lateral profiles were normalized to their central axis value. For illustrational purposes every other calculated depth dose value is not shown in part (a) and (c).

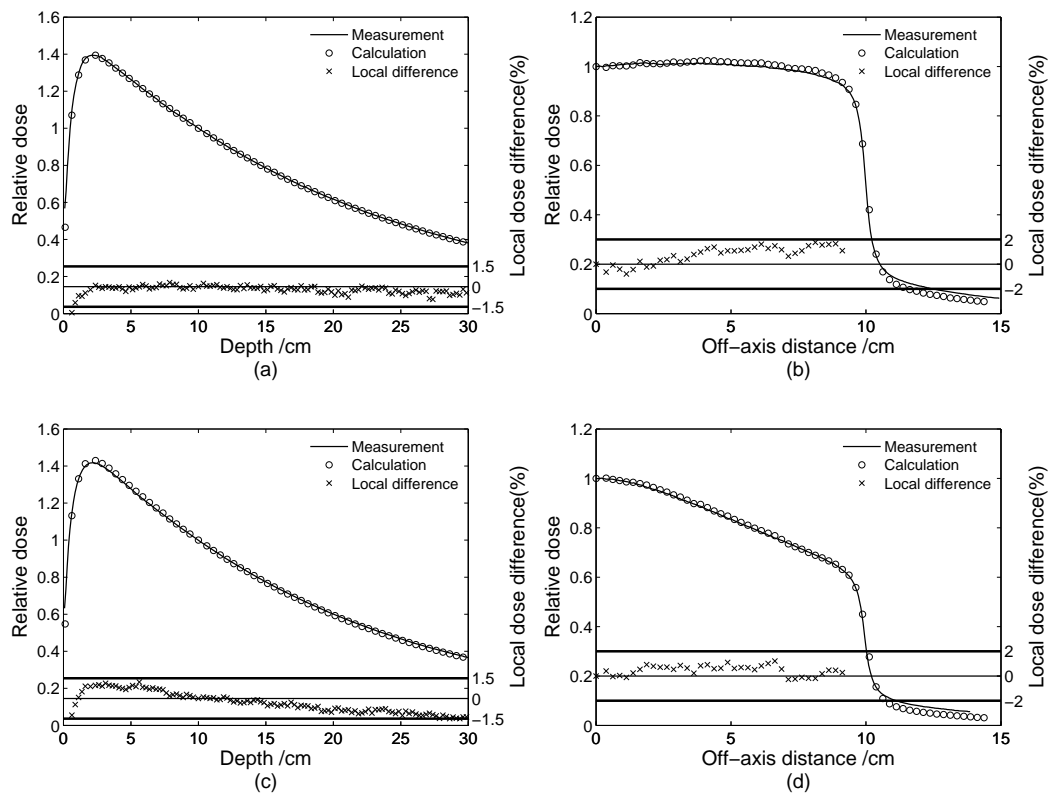


Figure 3. Comparisons of calculated and measured depth doses and lateral profiles at 10 MV. The difference between measured and calculated dose values is shown at the bottom of the figures (right scale). Left: Depth dose distribution for 10 MV beams with (a) and without (c) a flattening filter for a $10 \times 10 \text{ cm}^2$ field with SSD 90 cm. The depth dose data were normalized to unity at 10 cm depth. Right: Lateral profiles with (b) and without (d) a flattening filter at 10 cm depth at an SSD of 90 cm for a $20 \times 20 \text{ cm}^2$ field. Lateral profiles were normalized to their central axis value. For illustrational purposes every other calculated depth dose value is not shown in part (a) and (c).

3.2 Output

One potential advantage of removing the flattening filter is the increased dose rate, i.e. reduced treatment beam-on time. In figure 4, the ratio of dose per initial electron at points between the central axis and the field edge for beams with and without flattening filter are shown. The ratio was calculated at 10 cm depth in water at SSD 90 cm for a $20 \times 20 \text{ cm}^2$ field for both 6 MV and 10 MV beams. For a $10 \times 10 \text{ cm}^2$ field the dose rate at 10 cm depth on the central axis increased by a factor 1.76 and 2.66, for the 6 MV and 10 MV beams, respectively. Without any filter in the beam line the corresponding increase in dose rate were 2.23 and 3.23 times for the 6 MV and 10 MV beams, respectively.

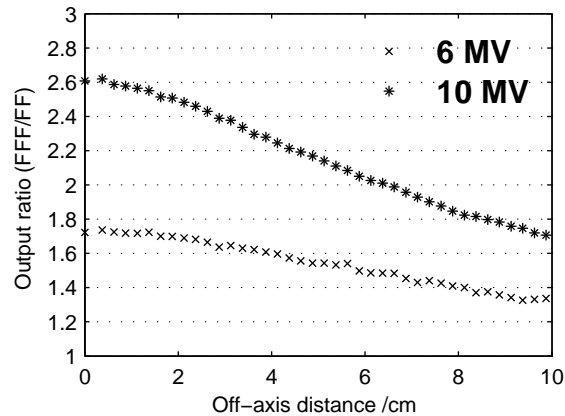


Figure 4. Output ratio (FFF/FF) variations with off-axis position for 6 MV and 10 MV at 10 cm depth in water for a 20x20 cm² field at SSD 90 cm. The uncertainty in the calculations was below 1 % (1 SD).

3.3 Spectra

In figure 5, the photon spectra at the central axis and at the field edge are presented for the 6 MV and 10 MV beams with a field size of 40x40 cm² at an SSD of 100 cm. It clearly shows an increased amount of high energy photons in the central part of the beam compared to at the field edge, when using a flattening filter. This effect is much less pronounced in flattening filter-free mode. The mean energy at the central axis and at the field edge for the examined beams is presented in table 1.

Table 1. Mean energy at the central axis and at an off-axis distance of 17-18 cm. The mean energy was calculated in a plane normal to the beam axis 100 cm from the target with a field size of 40x40 cm².

	Mean energy at central axis (MeV)	Mean energy at field edge (MeV)
6 MV, FF	1.96	1.50
6 MV, FFF	1.65	1.50
10 MV, FF	2.96	2.37
10 MV, FFF	2.37	2.10

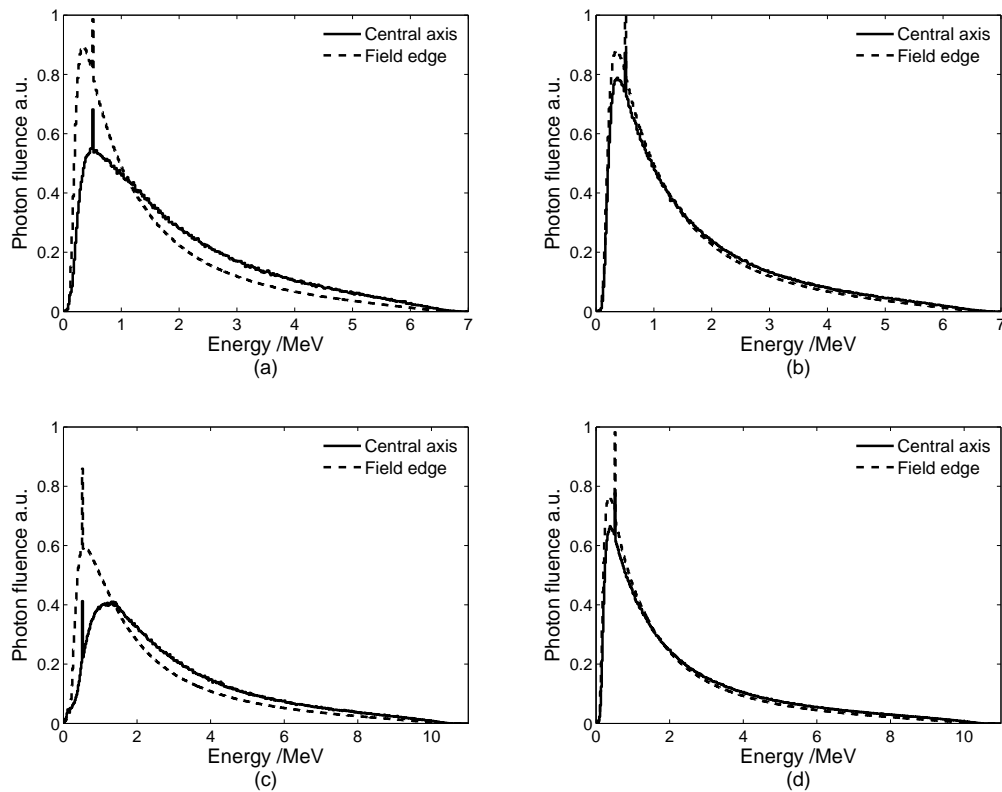


Figure 5. Photon fluence spectra in air, normalized per unit total fluence, for 6 MV beams with (a) and without (b) a flattening filter and 10 MV beams with (c) and without (d) a flattening filter. Data was sampled in a plane normal to the central axis at 100 cm distance from the target for a 40x40 cm² field. The lateral spectra (dotted line) are sampled at 17-18 cm distance from the central axis.

3.4 Mean energy, HVL

The variation of mean energy is also displayed as the lateral variation of HVL in figure 6 together with the generic fit from Tailor *et al* (1998). In these figures, Monte Carlo calculated values are also compared to the measured values from Georg *et al* (2010). The HVL ratios agree within 1.5 % for all examined beams between measurements and Monte Carlo calculations. The absolute HVL values agree within 0.4 cm for the 6 MV beam and within 1.2 cm for the 10 MV beam.

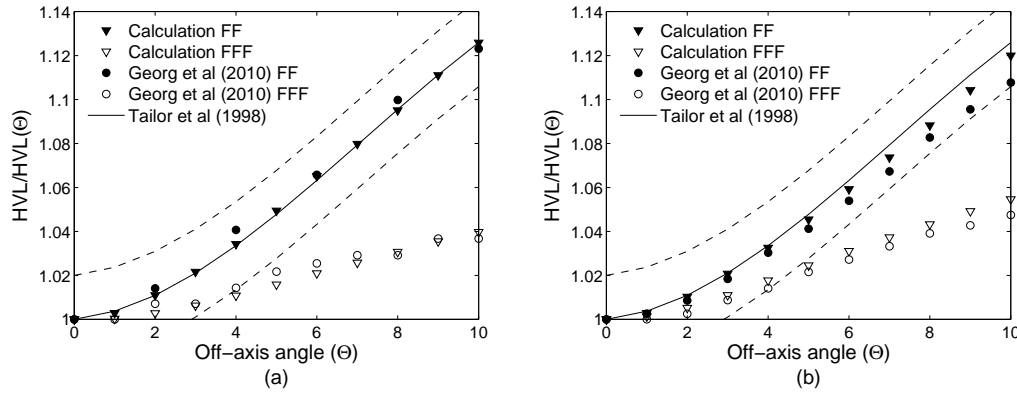


Figure 6. The half-value layer (HVL) at off-axis angles normalized to the HVL at the central axis for 6 MV (a) and 10 MV (b). Measurements, Monte Carlo calculations and values from the Tailor equation are shown for flattened beams (FF) and flattening filter-free beams (FFF). The dotted lines represent a $\pm 2\%$ deviation from the fit in Tailor *et al* (1998).

3.5 Origin of particles

To illustrate the origin of the head scatter contribution for the investigated beams, the last interaction point of photons along the central axis reaching the scoring plane inside the field edges is presented as a frequency distribution in figure 7. The dotted line shows this distribution for flattening filter-free mode and the solid line is for the conventional beam. In the figure the different parts of the accelerator head can be identified, starting off with the high peak to the far left indicating the target, then the primary collimator, filter, monitor chamber, backscatter plate and the secondary collimators to the far right. Since the entire filter carousel and filter holder are modelled, and they are the same in both configurations, the corresponding parts of the diagram representing the filter are geometrically equal. However, note that the scale of the y-axis is logarithmic and the differences between the two modes are large. The total amount of photon scatter from the accelerator head was reduced by $(31.7 \pm 0.03)\%$ for the 6 MV beam and $(47.6 \pm 0.02)\%$ for the 10 MV beam in flattening filter-free mode. The amount of scatter from the secondary collimators was reduced by $(27.7 \pm 0.1)\%$ and $(40.4 \pm 0.05)\%$ for the 6 MV and 10 MV beams, respectively. The reduction of scatter from the filter including the filter carousel was $(48.8 \pm 0.03)\%$ and $(65.6 \pm 0.01)\%$. The filter does, however, still account for about 40% of the scattered radiation in flattening filter-free mode, as opposed to around 50% in conventional mode. The uncertainty values presented represent the statistical uncertainty (1 SD) in the simulations.

In figure 8, the ratios of photons having interacted in the flattening filter or copper plate to the total photon fluence in air are shown with off-axis distance. For the 6 MV beam, $(5.51 \pm 0.02)\%$ of the total photons reaching the central-axis at 100 cm distance from the target have interacted in the flattening filter. In flattening filter-free mode only $(2.12 \pm 0.02)\%$ of the photons interacted in the copper plate. The corresponding values for the 10 MV beam are $(7.56 \pm 0.01)\%$ for the conventional beam and

(1.84 ± 0.01) % for the flattening filter-free beam. At 5 cm outside the field edge these ratios becomes larger. For the 6 MV beam (58.35 ± 0.09) % and (49.13 ± 0.11) % of the photons have interacted in the flattening filter or copper plate for the FF and FFF beams, respectively. For the 10 MV beams these ratios were (56.57 ± 0.04) % and (47.23 ± 0.04) % for the FF and FFF beams.

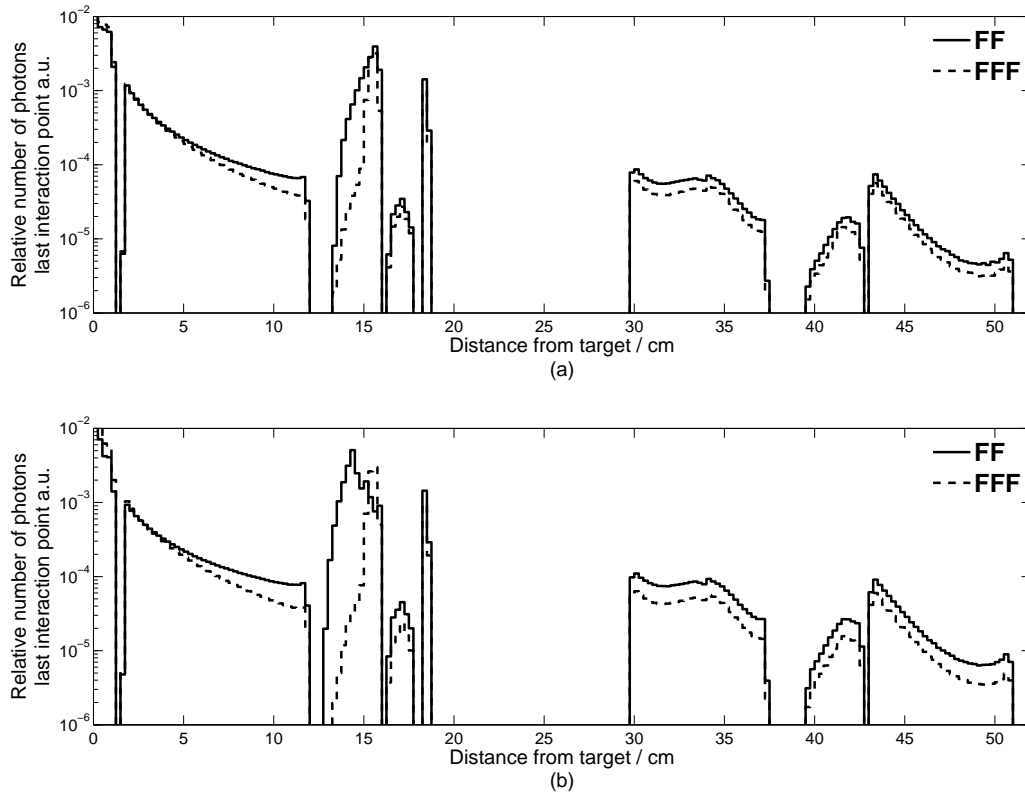


Figure 7. Relative number of photons for 6 MV (a) and 10 MV (b) produced along the beam axis reaching the scoring plane at isocenter, i.e. 100 cm, for a $20 \times 20 \text{ cm}^2$ field. Dotted lines represent flattening filter-free beams and solid lines represent conventional beams. The peak to the far left, representing the target, has been cut for illustrational purposes.

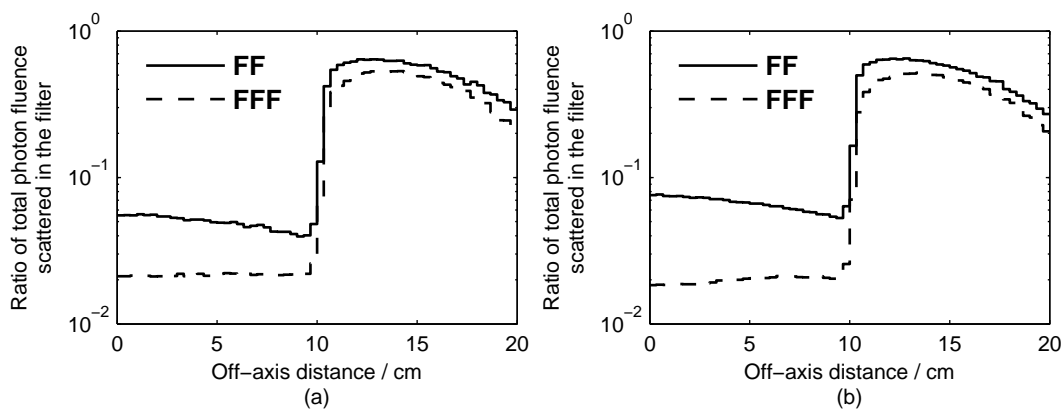


Figure 8. Ratios of photons having interacted in the flattening filter or copper plate for the 6 MV (a) and 10 MV (b) beams. The ratios were calculated in a scoring plane at isocenter, i.e. SSD 100 cm, for a 20x20 cm² field and the LATCH variable in the BEAMnrc system was used to extract the interaction history of the photons. Dotted lines represent flattening filter-free beams and solid lines represent conventional beams.

4. Discussion

The tuning procedure resulted in a good agreement between measurements and the Monte Carlo calculations. The agreement in the penumbral region was better for the 10 MV beam. This could partly be explained by the different measurement devices used. The 10 MV beam profiles shown were measured using a SFD-diode with a smaller active region than the diode used for the 6 MV beam. The differences outside the field edge for the 10 MV beam are also mainly explained by this since the unshielded SFD-diode gives an over response outside the field compared to ion chamber measurements.

One of the often pointed out advantages of removing the flattening filter is the increased output. In this study the output per incident electron hitting the target at 10 cm depth was increased by 1.76 and 2.66 times for 6 MV and 10 MV, respectively. This is a slightly larger increase than the measured factors 1.68 and 2.30 at the same depth reported by Kragl *et al* (2009) and can most likely be explained by dose rate related settings of the accelerator when performing the measurements. The increase is smaller than previously reported by Mesbahi *et al* (2007) and Cashmore (2008) for 6 MV beams at the depth of maximum dose from an Elekta linac since they did not include a copper filter in their simulations and measurements. When removing the copper plate, the dose rate for the 6 MV beam at 10 cm depth and a field size of 10x10 cm² was 2.23 in this study with is slightly larger than the 2.17 times increase reported by Mesbahi *et al* (2007). This difference is likely to be explained by the lower incident electron energy of 6.2 MeV in their study.

The spectra shown in figure 5 demonstrate a less pronounced off-axis beam softening for the flattening filter-free beams compared to the conventional ones. The altered energy composition of beams without flattening filter requires a new set of correction factors for reference dosimetry (Xiong and Rogers 2008, Ceberg *et al* 2010). The different spectra and their lateral variation are also reflected in the HVL data and their variation. The effect of less spectral variation with off axis distance is responsible for the reduced variation of lateral profiles at different depth (Vassiliev *et al* 2006, Kragl *et al* 2009).

There are clearly fewer photons being scattered in the main components of the collimator head in flattening filter-free mode, since a large portion of the scattering material in the beam has been removed. Even so, the copper plate inserted in the flattening filter-free mode still accounts for a large portion of the head scatter. The scatter contribution from the primary collimator is also almost constant

for the two modes. An obviously reduced proportion of the total photon fluence in air is originating from photons that have been interacting in the flattening filter. Due to the different designs of the flattening filters for the 6 MV and 10 MV beams the reduction was larger for the 10 MV beam, since the copper plate used in flattening filter-free mode are identical for the two energies.

In the interest of maximizing the dose rate on the central axis and minimizing the unwanted scatter dose outside the field, it would therefore be advantageous to decrease the thickness of the replacement filter. However, the thickness of this filter is also dependent on safety concerns and beam-steering properties, and there is a trade-off between these contradictory requirements.

The introduction of a copper plate in the beam line facilitates the steering of the beam by removing scatter from the primary collimator and thus preventing saturation of the monitor chamber. Another possible effect of this metal plate is that it produces electrons, which will give a higher signal to the monitor chamber, needed for the steering (Cashmore 2008).

5. Conclusions

A Monte Carlo model has been built and validated by measurements for a linear accelerator beam operating with and without flattening filter. The calculations showed good agreement with measurements for both delivery modes. It has also been demonstrated that the off-axis softening effect was much less pronounced without the flattening filter, and the results were in very good agreement with previous experimental results. This property is the reason for the reduced variation in lateral profiles measured at different depth (Vassiliev *et al* 2006, Kragl *et al* 2009). Finally, we studied the composition of the head-scattered photons. It was concluded from our Monte Carlo simulations that, although the flattening filter-free beam produces less scattered radiation, the replacement filter stands for a large portion of the head scatter.

Acknowledgements

The authors wish to thank Kevin Brown from ELEKTA oncology systems for his R&D and engineering support related to this study in order to modify and tune the accelerators.

References

- Araki F 2006 Monte Carlo study of a Cyberknife stereotactic radiosurgery system *Med. Phys.* **33** 2955-63
- Cashmore J 2008 The characterization of unflattened photon beams from a 6 MV linear accelerator *Phys. Med. Biol.* **53** 1933-46

- Chaney E L, Cullip T J and Gabriel T A 1994 A Monte Carlo study of accelerator head scatter *Med. Phys.* **21** 1383-90
- Ceberg C, Johnsson S, Lind M and Knoos T 2010 Prediction of stopping-power ratios in flattening-filter free beams *Med. Phys.* **37** 1164-8
- De Smedt B, Raynaert N, Flachet F, Coghe M, Thompson M G, Paelinck L, Pittomvils G, De Wagter C, De Neve W and Thierens H 2005 Decoupling initial electron beam parameters for Monte Carlo photon beam modelling by removing beam-modifying filters from the beam path *Phys. Med. Biol.* **50** 5935-51
- Fix M K, Stampanoni M, Manser P, Born Ernst J, Mini R and Ruegsegger P 2001 A multiple source model for 6 MV photon beam dose calculations using Monte Carlo *Phys. Med. Biol.* **46** 1407-27
- Georg D, Kragl G, Wetterstedt S, McCavana P, McClean B and Knoos T 2010 Photon beam quality variations of a flattening filter free linear accelerator *Med. Phys.* **37** 49-53
- Hall E J 2006 Intensity-modulated radiation therapy, protons, and the risk of secondary cancers *Int. J. Radiat. Oncol. Biol. Phys.* **65** 1-7
- Hubbell J H and Seltzer S M 1995 Tables of x-ray mass attenuation coefficients and mass energy-absorption coefficients from 1 keV to 20 keV for elements $z = 1$ to 92 and 48 additional substances of dosimetric interest *NISTIR 5632*
- Jeraj R, Mackie T R, Balog J, Olivera G, Pearson D, Kapatoes J, Ruchala K and Reckwerdt P 2004 Radiation characteristics of helical tomotherapy *Med. Phys.* **31** 396-404
- Kawrakow I and Rogers D W O 2003 The EGSnrc Code System: Monte Carlo Simulation of Electron and Photon Transport *Technical Report PIRS-701* (Ottawa, Canada: National Research Council of Canada)
- Kragl G, af Wetterstedt S, Knausl B, Lind M, McCavana P, Knoos T, McClean B and Georg D 2009 Dosimetric characteristics of 6 and 10MV unflattened photon beams *Radiother. Oncol.* **93** 141-6
- Kragl G, Baier F, Lutz S, Albrich D, Dalaryd M, Kroupa B, Wiezorek T, Knöös T and Georg D 2010 Flattening filter free beams in SBRT and IMRT: dosimetric assessment of peripheral doses *Z. Med. Phys.* **Article in press** (doi:10.1016/j.zemedi.2010.07.003)
- Kry S F, Vassiliev O N and Mohan R 2010 Out-of-field photon dose following removal of the flattening filter from a medical accelerator *Phys. Med. Biol.* **55** 2155-66
- Mackie T R, Holmes T, Swerdloff S, Reckwerdt P, Deasy J O, Yang J, Paliwal B and Kinsella T 1993 Tomotherapy: a new concept for the delivery of dynamic conformal radiotherapy *Med. Phys.* **20** 1709-19
- Mesbahi A, Mehnati P, Keshtkar A and Farajollahi A 2007 Dosimetric properties of a flattening filter-free 6-MV photon beam: a Monte Carlo study *Radiat. Med.* **25** 315-24

- Mesbahi A and Nejad F S 2008 Monte Carlo study on a flattening filter-free 18-MV photon beam of a medical linear accelerator *Radiat. Med.* **26** 331-6
- O'Brien P F, Gillies B A, Schwartz M, Young C and Davey P 1991 Radiosurgery with unflattened 6-MV photon beams *Med. Phys.* **18** 519-21
- Pönisch F, Titt U, Vassiliev O N, Kry S F and Mohan R 2006 Properties of unflattened photon beams shaped by a multileaf collimator *Med. Phys.* **33** 1738-46
- Rogers D W O, Faddegon B A, Ding G X, Ma C-M, Wei J and Mackie T R 1995 BEAM: A Monte Carlo code to simulate radiotherapy treatment units *Med. Phys.* **22** 503-24
- Rogers D W O, Walters B and Kawrakow I 2005 BEAMnrc Users Manual *NRC Report PIRS 509(a)revI*
- Sheikh-Bagheri D and Rogers D W O 2002 Sensitivity of megavoltage photon beam Monte Carlo simulations to electron beam and other parameters *Med. Phys.* **29** 379-90
- Taylor R C, Tello V M, Schroy C B, Vossler M and Hanson W F 1998 A generic off-axis energy correction for linac photon beam dosimetry *Med. Phys.* **25** 662-7
- Xiong G and Rogers D W O 2008 Relationship between $\%dd(10)_x$ and stopping-power ratios for flattening filter free accelerators: A Monte Carlo study *Med. Phys.* **35** 2104-9
- Titt U, Vassiliev O N, Pönisch F, Dong L, Liu H and Mohan R 2006 A flattening filter free photon treatment concept evaluation with Monte Carlo *Med. Phys.* **33** 1595-602
- Vassiliev O N, Kry S F, Kuban D A, Salehpour M, Mohan R and Titt U 2007 Treatment-planning study of prostate cancer intensity-modulated radiotherapy with a Varian Clinac operated without a flattening filter *Int. J. Radiat. Oncol. Biol. Phys.* **68** 1567-71
- Vassiliev O N, Titt U, Kry S F, Pönisch F, Gillin M T and Mohan R 2006 Monte Carlo study of photon fields from a flattening filter-free clinical accelerator *Med. Phys.* **33** 820-7
- Vassiliev O N, Titt U, Kry S F, Pönisch F, Gillin M T and Mohan R 2006 Monte Carlo study of photon fields from a flattening filter-free clinical accelerator *Med. Phys.* **33** 820-7
- Walters B, Kawrakow I and Rogers D W O 2005 DOSXYZnrc Users Manual *NRC Report PIRS 794 rev B*